THE JOURNAL OF BIOLOGICAL CHEMISTRY VOL. 286, NO. 19, pp. 16734–16742, May 13, 2011

Crystal Structure of the Outer Membrane Protein RcsF, a New Substrate for the Periplasmic Protein-disulfide Isomerase DsbC*[S]

Received for publication, February 15, 2011, and in revised form, March 7, 2011 Published, JBC Papers in Press, March 16, 2011, DOI 10.1074/jbc.M111.224865

Pauline Leverrier[‡§¶1,2], Jean-Paul Declercq[‖1], Katleen Denoncin[‡§¶3], Didier Vertommen[‡4], Annie Hiniker[**], Seung-Hyun Cho[‡§¶], and Jean-François Collet[‡§¶5]

*From [§]Welbio (Walloon Excellence in Life Sciences and Biotechnology), [‡]de Duve Institute, Université Catholique de Louvain, B-1200 Brussels, Belgium, [¶]Brussels Center for Redox Biology, B-1200 Brussels, Belgium, the [‖]Institute of Condensed Matter and Nanosciences, Université Catholique de Louvain, B-1348 Louvain-la-Neuve, Belgium, and the **Department of Molecular Biology, Princeton University, Princeton, New Jersey 08544*

The bacterial Rcs phosphorelay is a stress-induced defense mechanism that controls the expression of numerous genes, including those for capsular polysaccharides, motility, and virulence factors. It is a complex multicomponent system that includes the histidine kinase (RcsC) and the response regulator (RcsB) and also auxiliary proteins such as RcsF. RcsF is an outer membrane lipoprotein that transmits signals from the cell surface to RcsC. The physiological signals that activate RcsF and how RcsF interacts with RcsC remain unknown. Here, we report the three-dimensional structure of RcsF. The fold of the protein is characterized by the presence of a central 4-stranded β sheet, which is conserved in several other proteins, including the copper-binding domain of the amyloid precursor protein. RcsF, which contains four conserved cysteine residues, presents two nonconsecutive disulfides between Cys^{74} and Cys^{118} and between Cys^{109} and Cys^{124}, respectively. These two disulfides are not functionally equivalent; the Cys^{109}–Cys^{124} disulfide is particularly important for the assembly of an active RcsF. Moreover, we show that formation of the nonconsecutive disulfides of RcsF depends on the periplasmic disulfide isomerase DsbC. We trapped RcsF in a mixed disulfide complex with DsbC, and we show that deletion of *dsbC* prevents the activation of the Rcs phosphorelay by signals that function through RcsF. The three-dimensional structure of RcsF provides the structural basis to understand how this protein triggers the Rcs signaling cascade.

The envelope of Gram-negative bacteria is a complex macromolecular structure that serves as a permeability barrier protecting bacterial cells from ever-changing environmental conditions (1–3). To maintain envelope integrity, Gram-negative bacteria have evolved complicated signaling systems that allow them to react to a range of envelope stresses by modulating the expression of specific genes. Several envelope stress response systems have been described in *Escherichia coli*, including the Rcs phosphorelay (4, 5).

The Rcs signaling cascade was first identified by its role in the transcriptional regulation of genes involved in the biosynthesis of colanic acid in *E. coli* (6). Colanic acid is a capsule polysaccharide that is produced by bacteria in response to envelope perturbations, osmotic stress, and growth on surfaces (7). Production of colanic acid leads to the formation of a mucoid layer on the bacterial cell surface, which results in a distinctive mucoid phenotype (see Fig. 4). In addition to its role in controlling capsule synthesis, the Rcs phosphorelay is required for normal biofilm formation, contributes to antibiotic resistance, and regulates virulence-associated structures involved in motility and host recognition (8–10).

The Rcs phosphorelay is a complex signaling pathway that includes three proteins, RcsC, RcsD, and RcsB (9, 11). RcsC is an inner membrane sensor protein that presents an N-terminal histidine kinase domain and a C-terminal receiver domain (12). In response to environmental signals, RcsC is predicted to autophosphorylate a conserved histidine residue located in the kinase domain. The phosphoryl group is then transferred to a conserved aspartate residue present in the receiver domain (9, 13). RcsD, which is also located in the inner membrane, contains a histidine-containing phosphotransmitter domain (Hpt), which mediates phosphoryl transfer between the receiver domain of RcsC and an aspartate residue located in the receiver domain of RcsB, a cytoplasmic response regulator (14). Phosphorylation of RcsB allows this cytoplasmic protein to bind to target promoters on the chromosomal DNA via a DNA-binding domain (9, 15).

In addition to RcsC, RcsD, and RcsB, the Rcs phosphorelay involves auxiliary proteins that are required for the normal functioning of the system (9, 11). In *E. coli*, the best characterized auxiliary proteins are RcsA and RcsF. RcsA is an unstable cytoplasmic protein that belongs to the same family of tran-

* This work was supported by the Interuniversity Attraction Pole Programme-Belgian Science Policy, Network P6/05 (to J.-F. C.), and by grants from the Fonds de la Recherche Scientifique-Fonds National de la Recherche Scientifique (to J.-F. C.).

[S] The on-line version of this article (available at http://www.jbc.org) contains supplemental Tables S1 and S2, Figs. S1 and S2, and additional references.

The atomic coordinates and structure factors (code 2y1b) have been deposited in the Protein Data Bank, Research Collaboratory for Structural Bioinformatics, Rutgers University, New Brunswick, NJ (http://www.rcsb.org/).

[1] Both authors contributed equally to this work.

[2] Chargée de Recherche.

[3] Research fellow of the Fonds pour la Formation à la Recherche dans l'Industrie et dans l'Agriculture.

[4] Collaborateur Logistique.

[5] Chercheur Qualifié of the Fonds de la Recherche Scientifique-Fonds National de la Recherche Scientifique. To whom correspondence should be addressed: 75-39 Av. Hippocrate, 1200 Brussels, Belgium. Tel.: 32-2-764-75-62; Fax: 32-2-764-75-98; E-mail: jfcollet@uclouvain.be.

scriptional regulators as RcsB (16). RcsA interacts with phosphorylated RcsB to form a heterodimer that binds to the promoters of a subset of Rcs-regulated genes, including those involved in capsule synthesis (17, 18).

RcsF is a small lipoprotein (14 kDa) anchored in the outer membrane and oriented toward the periplasm (19). RcsF was first identified by its ability to induce the Rcs phosphorelay when overexpressed (20), an activation that is dependent on RcsC (21). The function of RcsF is to transduce signals that this protein perceives in the outer part of the envelope to RcsC (9). For instance, treatments that alter the integrity of the outer membrane, such as exposure to cationic antimicrobial peptides (22), or that target the peptidoglycan layer, like exposure to lysozyme (23) or β-lactam antibiotics (10), activate the Rcs phosphorelay. This induction has been shown to be dependent on RcsF (19). Moreover, mutations that lead to defects in the envelope, such as mutations in the lipopolysaccharide synthesis pathway or in *mdoG* and *mdoH*, two genes that are involved in the synthesis of membrane-derived oligosaccharides, also activate the Rcs cascade in an RcsF-dependent manner (19, 24).

Despite the important role played by the Rcs phosphorelay in monitoring envelope integrity, in biofilm formation, and in bacterial virulence, we still have a poor understanding of the molecular mechanisms that activate the system and control its correct functioning. In particular, the physiological signals that turn on the Rcs phosphorelay remain unknown, and how the outer membrane protein sensor RcsF transfers environmental signals to RcsC is not understood.

The Rcs phosphorelay has been mostly studied using bacterial genetics. To elucidate how this system works and to understand the molecular mechanisms that control its activity, biochemical and structural data are required.

Here, we report the three-dimensional crystal structure of the sensor protein RcsF. The protein fold is characterized by the presence of a central four-stranded β sheet. Two nonconsecutive disulfides, including one cross-strand disulfide, are present in the structure. We show that formation of these disulfides involves the periplasmic protein-disulfide isomerase DsbC. Our work provides the structural and biochemical basis that should facilitate the understanding of the mechanism used by RcsF to transmit signals across the periplasm.

EXPERIMENTAL PROCEDURES

Bacterial Strains and Growth Conditions—The bacterial strains used in this study are listed in supplemental Table S1. All the strains are derivatives of the *E. coli* K-12 strain MC4100 (25). Cells were grown aerobically in either LB or M63 minimal media. Unless otherwise indicated, M63 minimal medium was supplemented with 0.2% glucose, vitamins, 1 mM $MgSO_4$, and a mixture of amino acids. When necessary, growth media were supplemented with either chloramphenicol (25 μg/ml), kanamycin (50 μg/ml), or ampicillin (200 μg/ml). All alleles were moved by bacteriophage P1 transduction using standard procedures (26). The resistance cassette was removed from the chromosome by using the pCP20 plasmid encoding the FLP recombinase (27).

Construction of the Expression Plasmids—The genomic DNA of *E. coli* MC4100 was used as a template for the PCR. The primers are listed in supplemental Table S2. The PCR amplifications were performed using *Pfu* DNA polymerase (Fermentas), and samples were subjected to 25 cycles of 30 s denaturation at 95 °C, 30 s annealing at 55 °C, and 3 min elongation at 68 °C, followed by 5 min at 68 °C. The *rcsF* gene, without the sequence corresponding to the signal peptide and the lipobox, was amplified using *rcsF* Fw1 as forward primer (containing an NcoI site, CCATGG) and *rcsF* Rv1 as reverse primer (containing an XhoI site, CTCGAG) (see supplemental Table S2 for primers list). The PCR product was analyzed by electrophoresis on a 1% agarose gel and stained with ethidium bromide. It was then purified, double-digested, and ligated into the plasmid pET28a (Novagen) for expression of the protein with a C-terminal His tag and no N-terminal His tag (the sequence of the recombinant protein is provided supplemental Table S2). For expression of RcsF in the periplasm using the OmpA signal sequence, the *rcsF* gene, without the sequence corresponding to the first 16 residues, was amplified using *rcsF* Fw2 (containing a KasI site, GGCGCC) as forward primer and *rcsF* Rv2 (containing an NcoI site, CCATGG) as reverse primer. The amplification product was then cloned into the pASK-IBA16 vector (IBA BioTAGnology®). The truncated version of *rcsF* starting at residue Pro^{48} ($RcsF_{trunc}$) was also cloned into the pASK-IBA16 vector, after PCR amplification using the primers $rcsF_{trunc}$ Fw and *rcsF* Rv2. The resulting plasmids (pET28a::*rcsF*, pASK-IBA16::*rcsF*, and pASK-IBA::$rcsF_{trunc}$) were first transformed into *E. coli* XLIBlue competent cells for sequencing. pET28a::*rcsF* was then transformed into Rosetta-Gami BL21 (New England Biolabs)-competent cells for expression of RcsF in the oxidizing cytoplasm of that strain. pASK-IBA16::*rcsF* and pASK-IBA16::$rcsF_{trunc}$ were transformed in different MC4100 background for phenotypic characterization.

Site-directed Mutagenesis—The QuikChange mutagenesis kit (Stratagene) was used for the generation of the RcsF mutants in which the cysteine residues are replaced by serines. The plasmid pASK-IBA16::*rcsF* was used as a template. The forward and reverse primers that were used are listed in supplemental Table S2. The PCR amplification reaction was performed using *Pfu* DNA polymerase, and samples were subjected to 20 cycles of 30 s denaturation at 95 °C, 30 s annealing at 55 °C, and 9 min elongation at 68 °C, followed by a 11-min step at 68 °C. The DpnI restriction enzyme was used to digest the parental supercoiled double-stranded DNA. The plasmids harboring the sequence of the mutated proteins were transformed into *E. coli* XLIBlue competent cells for sequencing and then in PL262 (*rcsF*::kan) competent cells for phenotypic characterization.

Expression and Purification of the Recombinant RcsF Protein—Rosetta-Gami BL21 cells transformed with the pET28a::*rcsF* expression plasmid were grown at 37 °C in 4 liters of LB medium containing ampicillin (200 mg/liter) and kanamycin (50 mg/liter) to an A_{600} of 0.6. Isopropyl 1-thio-β-D-galactopyranoside (0.5 mM) was then added to induce expression during 3 h with shaking. The cells were harvested by centrifugation, and the cell pellet was resuspended in 20 ml of a buffer containing NaP_i, pH 8.0, 100 mM and NaCl 0.3 M (Buffer A). The cells were then disrupted using a French press. After centrifugation (40 min, 18,000 × *g*), the supernatant was diluted three times

and loaded onto a Ni-NTA[6] chromatography column equilibrated with Buffer A. Elution was performed by applying a linear gradient of imidazole (from 30 to 300 mM) in Buffer A, and the eluted fractions were analyzed by SDS-PAGE containing 16% (v/v) acrylamide. The protein was ≈99% homogeneous after this step.

Crystallization, Data Collection, and Processing—Before crystallization, the protein solution at a concentration of 11 mg/ml was mixed with 5-amino-2,4,6-triiodoisophthalic acid (I3C) neutralized with LiOH to reach a concentration of 20 mM. All attempts to grow crystals in the absence of I3C were completely unsuccessful. Furthermore, the replacement of I3C with 5-amino-2,4,6-tribromoisophthalic acid (the same compound with three bromo atoms instead of the three iodine atoms) did not produce any crystals. The incorporation of the I3C compound known as the "magic triangle" (28) initially aimed at providing a way to obtain phases by single wavelength anomalous dispersion, but it turned out to be an essential ligand for crystal growth. Crystals for data collection were grown by vapor diffusion using the hanging drop method at 18 °C. The well solution (500 μl) consisted of 1.8 M ammonium sulfate, 0.1 M sodium acetate, pH 4.5, and 0.02% (w/v) sodium azide. The drop was formed by mixing 1 μl of the protein + I3C mixture with 1 μl of the well solution. Crystals appeared after several weeks.

Before data collection, crystals were soaked for a few seconds in a solution similar to the mother liquor but containing 20% (w/v) glycerol as cryo-protectant and flash-cooled at 100 K. Data were collected on beamline X12 at EMBL, DESY. Two data sets were collected. The first data set was collected at a long wavelength with a high level of redundancy, to obtain a good anomalous signal from the iodine atoms for phasing using the single wavelength anomalous dispersion method. For the second data set, a shorter wavelength was used and was allowed to reach a higher resolution for the refinement. The diffraction images were processed and merged with the XDS program package (29). The crystals are trigonal, space group $P3_121$, with one molecule in the asymmetric unit. Statistics of data collection and processing are given in Table 1.

The structure was solved by the single wavelength anomalous dispersion method applied to data set 1 using the Auto-Rickshaw procedure (30). The resulting model was refined against the high resolution data (data set 2) using REFMAC5 (31) of the CCP4 suite (32) and was manually completed and corrected using COOT (33). The final structure contains residues 48–131 of the protein chain, 46 water molecules, 1 sulfate ion, and 1 I3C molecule. Some statistics related to the refinement are given in Table 1.

Coordinates and Structure Factors—Atomic coordinates and structure factors have been deposited in the PDB with accession code 2y1b.

Trapping and Purification of the DsbC-RcsF Complex—A 1-liter LB culture of the *dsbC* strain carrying pBAD33::*dsbC*$_{CXXS}$ was grown at 25 °C to an A_{600} of 0.6. Expression was induced for 5 h by the addition of 0.2% L-arabinose. Proteins were precipitated using trichloroacetic acid (TCA) (10%) and resuspended in 25 ml of NaP_i, pH 8, 100 mM, NaCl 300 mM, SDS 0.3%, urea 8 M, and iodoacetamide 100 mM to prevent any further disulfide bond rearrangement. The lysate was centrifuged at 15,000 × *g* for 45 min. After incubation (overnight at room temperature) of the cleared mixture with 2 ml of Ni-NTA resin (Qiagen), a 1-ml column was packed with the protein-Ni-NTA resin complex and was washed thoroughly using NaP_i, pH 8, 100 mM, NaCl 300 mM, and SDS 0.3%. Elution of the complexes involving DsbC$_{CXXS}$ was performed using a step gradient from 30 to 300 mM imidazole. Only one fraction eluted from the column, which was concentrated 10-fold and analyzed by SDS-PAGE with or without DTT. After electrophoresis, the proteins were transferred to a nitrocellulose membrane and probed with an anti-RcsF antibody (1:3000) produced from a rabbit immunized with the purified protein (Eurogentec). Anti-rabbit IgG (Sigma) was used as the secondary antibody at a 1:5000 dilution. Thermo Scientific Pierce ECL Western blotting substrate and Fuji film were used to visualize the protein bands.

Mass Spectrometry—Intact mass measurement of RcsF was done by diluting the purified protein with 50:50 acetonitrile/water containing 0.1% formic acid to an approximate concentration of 5 μM. The sample was introduced by off-line infusion using a capillary electrospray at 1.5 μl/min. An LTQ XL mass spectrometer (LTQ XL, Thermo Fisher Scientific) was used to acquire mass spectra from *m*/*z* 400 to 2000 in centroid mode. Electrospray source conditions such as "source fragmentation" voltage and the tube lens voltage were optimized to help desolvation but without fragmenting the intact protein. Default values were used for most other data acquisition parameters. The resulting spectra were averaged up to 200 scans and were

TABLE 1
Data collection and refinement statistics

	Data set 1 (structure solution)	Data set 2 (refinement)
Wavelength	1.54975 Å	0.977910 Å
Space group	$P3_121$	$P3_121$
Unit cell		
a	56.14 Å	55.71 Å
c	61.81 Å	61.68 Å
Resolution range		
Overall (ov)	19.1 to 2.46	19.0 to 2.0
Highest shell (hs)	2.52 to 2.46	2.20 to 2.0
No. of reflections		
Total	87,651	27,634
Unique	7,889	7,786
Friedel pairs	Not merged	Merged
Completeness (ov/hs)	99.4/97.4%	99.6/99.6%
Rmerge (ov/hs)	0.083/0.377	0.082/0.522
$\langle I/\sigma(I)\rangle$ (ov/hs)	21.9/6.0	11.5/2.7
Refinement		
R-factor (ov/hs)		0.196/0.240
R_{free} (ov/hs)		0.258/0.330
Root mean square deviation from ideality		
Bonds		0.022 Å
Angles		2.16°
No. of water molecules		46
Mean *B* values		
Protein		30.3 Å^2
Water		37.4 Å^2
Sulfate		35.0 Å^2
I3C		34.1 Å^2

[6] The abbreviations used are: Ni-NTA, nickel-nitrilotriacetic acid; I3C, 5-amino-2,4,6-triiodoisophthalic acid; PDB, Protein Data Bank; CSD, cross-strand disulfide.

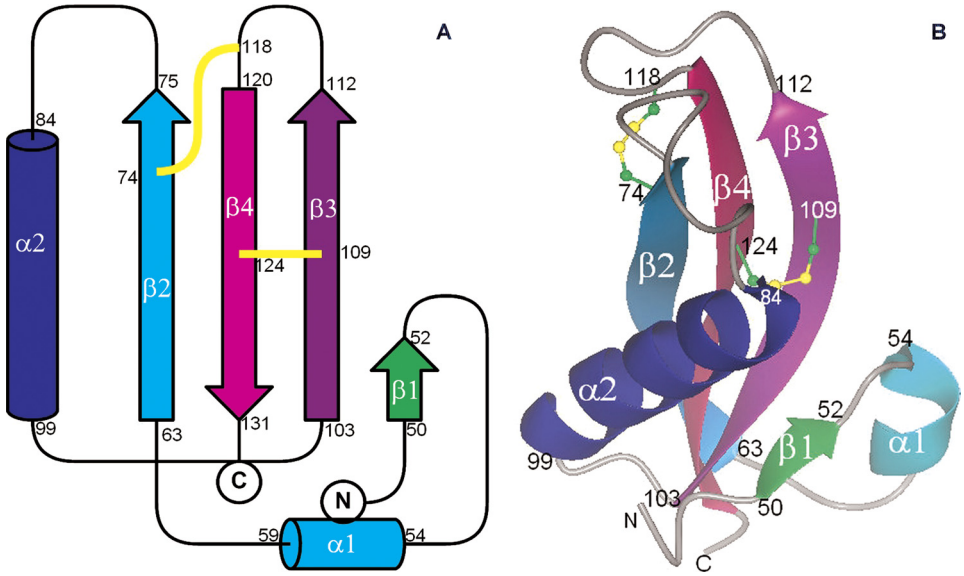

FIGURE 1. **Overall fold of the RcsF molecule.** The protein is colored from *green* (N terminus) to *pink* (C terminus). *A,* topological diagram on which the disulfide bonds are represented by a *yellow line*. The limits of the secondary structure elements are indicated. *B, ribbon diagram* in a more or less similar orientation. The side chains of the cysteine residues taking part in the disulfide bonds are drawn as *balls and sticks*. *A* was prepared with Topdraw (54) and *B* with CCP4mg (55).

deconvoluted using ProMass software (Thermo Fisher Scientific). We determined the mass of the protein used for crystallization to verify the sequence of the expression product.

In Vivo Expression Levels of RcsF—The bacterial strains were grown in minimal medium at 30 °C to an A_{600} of 0.8, and 1-ml samples were taken. Proteins were precipitated with 10% ice-cold TCA and centrifuged at 13,000 × *g* for 1 min. The pellets were washed with acetone, dried, and resuspended with 5× Laemmli buffer (SDS 10%, bromophenol blue 0.05%, glycerol 61%, Tris-HCl, pH 6.8, 300 mM). Standardized samples were analyzed by SDS-PAGE under nonreducing conditions. After electrophoresis, proteins were transferred to a nitrocellulose membrane and probed with an anti-RcsF antibody.

RESULTS

Three-dimensional Structure of RcsF—Here, we report the three-dimensional crystal structure of the RcsF protein sensor. The overall fold is illustrated in Fig. 1 and is characterized by the presence of a central four-stranded β sheet. One face of the β sheet is covered by a long α helix (α2), whereas the short helix α1 appears on the other side of the β sheet. After a search for a similar fold in the PDB using the DALI server (34), the best structural alignment corresponded to a protein of unknown function from the Gram-positive bacteria *Bacillus cereus* (PDB code 1vr4). 75 Cα atoms were superposed with a root mean square distance of 1.8 Å. A stereoscopic view of the superposition of the Cα traces of RcsF and code 1vr4 is shown in Fig. 2. The central β sheet and the α2 helix are well conserved. Two main differences are observed as follows: the α1 helix of RcsF has disappeared and is replaced by a loop in 1vr4 and the loop between β2 and α2 in RcsF is replaced in 1vr4 by an additional helix followed by a much longer loop. Other structural homologues of RcsF include a selenium-binding protein from *Methanococcus vannielii* (PDB code 2jz7), dodecin from *Halobacterium salinarum* (PDB code 2vx9-A), and the copper-binding domain of the Alzheimer peptide precursor protein (PDB code 2fma-A).

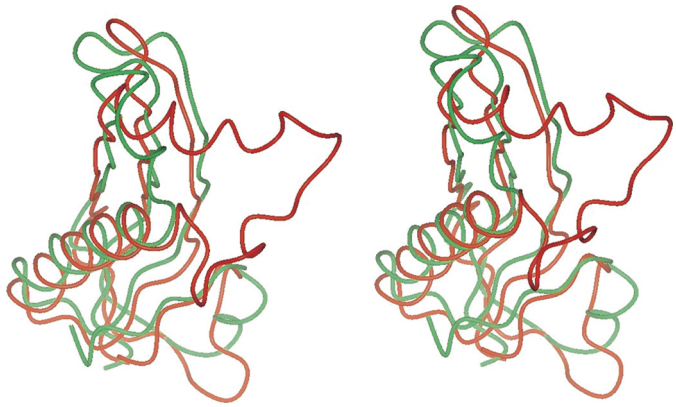

FIGURE 2. **Fold of RcsF is conserved in other proteins.** Stereoscopic view of a superposition of the Cα traces of RcsF (*green*) and PDB entry 1vr4 (*red*). The orientation is similar to that of Fig. 1*B*. This figure was prepared with CCP4mg (55).

Two disulfide bonds are observed in the structure. The first one between Cys^{74} and Cys^{118} links a residue in the β2 strand to a residue located in the β3-β4 loop. The second disulfide bond between Cys^{109} and Cys^{124} is a cross-strand disulfide (CSD) that links the β3 and β4 strands. Both disulfide bonds are illustrated in the electron density in Fig. 3.

I3C Ligand—As explained under "Experimental Procedures," the presence of the I3C ligand was essential for crystallization, suggesting that a strong interaction exists between this ligand and the protein. Indeed, we observed a close contact (3.05 Å) between one of the iodine atoms and the carbonyl oxygen atom of Pro^{82}. This interaction is nearly linear with a bond angle of 170.6° around the iodine atom and is usually described as "halogen bonding" (35, 36). On the aromatic ring of the I3C molecules, the two positions in ortho relative to this iodine atom are occupied by electron-attracting carboxylate groups that favor the appearance of a positive region on the

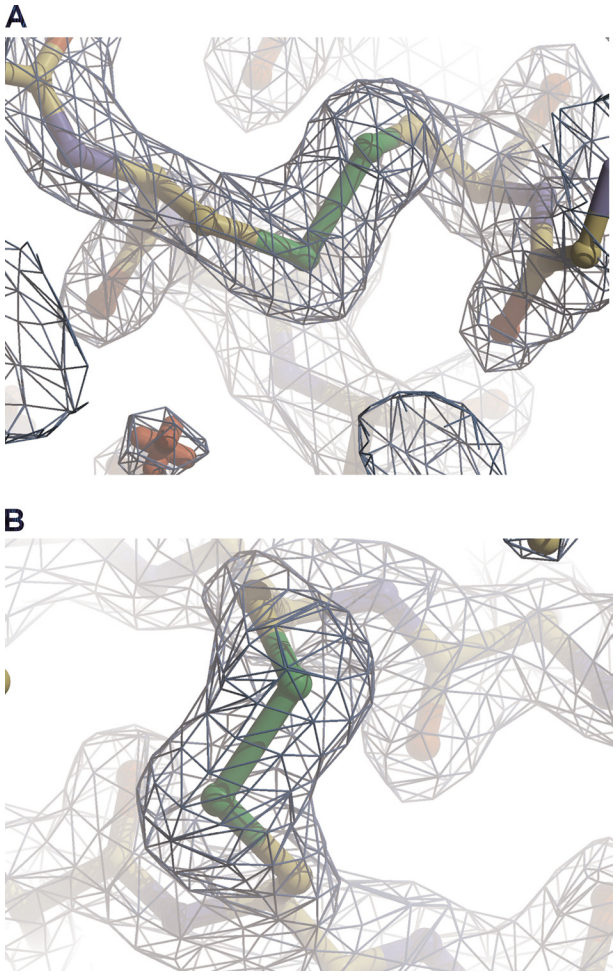

FIGURE 3. **RcsF presents two nonconsecutive disulfides.** The regions of the disulfide bond between Cys^{74} and Cys^{118} (*A*) and between Cys^{109} and Cys^{124} (*B*) are shown. The ($2mF_o - DF_c$) electron density map is contoured at a level of 1.5 σ. This figure was prepared with COOT (33).

outermost portion of the halogen surface. This phenomenon is known as a σ-hole and is responsible for the interaction with a nucleophile like the oxygen atom of a carbonyl group. One of the carboxylate groups is hydrogen-bonded to Ser^{84} Oγ.

N-terminal Segment of RcsF Is Disordered—The protein that was used for crystallization was expressed as a soluble protein containing a C-terminal His tag and lacking the first 16 residues corresponding to the signal peptide and the lipobox (remember that RcsF is a lipoprotein whose lipid moiety is anchored in the outer membrane). However, the observed electron density begins at residue Pro^{48}, suggesting that about 30 residues in the N-terminal part of the protein are completely disordered. The integrity of the sequence of the purified protein was confirmed using mass spectrometry to rule out any nonspecific proteolytic cleavage of the protein during expression and purification. The measured average mass was 13,609 ± 2 Da, which is in good agreement with a theoretical average mass of 13,612 Da taking into account the complete processing of the N-terminal methionine.

We then decided to determine whether the portion of RcsF that is not visible in the structure is important for the activity of the protein. It has been shown recently that expression of RcsF as a protein soluble in the periplasm constitutively induces the Rcs phosphorelay (22). Therefore, we decided to study the ability of a truncated version of the protein ($RcsF_{trunc}$), corresponding to residues Pro^{48} to Lys^{134}, to induce the Rcs phosphorelay when expressed in the periplasm, using strain mucoidity as a read-out. As explained in the Introduction, induction of the Rcs system leads to colanic acid production, which results in a distinctive mucoid phenotype. As indicated in Table 2, we observed that expression of $RcsF_{trunc}$ leads to a mucoid phenotype comparable with that observed when wild-type RcsF is expressed unanchored in the periplasm (supplemental Fig. S1). Thus, we can conclude from this experiment that the fraction of the polypeptide chain that is disordered in the crystal is not required for signaling, at least when RcsF is expressed as a soluble protein in the periplasm.

TABLE 2
Mucoid phenotype of strains expressing RcsF cysteine to serine mutants

The cysteine to serine RcsF mutants were expressed as soluble proteins in the periplasm of an *rcsF* deletion strain (PL262). Strains were grown on LB medium (containing ampicillin) for 2 days at room temperature.

Expressed protein		Mucoid phenotype
wtRcsF	CCCC	+++
$RcsF_{trunc}$	CCCC	+++
$RcsF_{C74S}$	SCCC	++
$RcsF_{C109S}$	CSCC	−
$RcsF_{C118S}$	CCSC	+++
$RcsF_{C124S}$	CCCS	−
$RcsF_{C74S/C118S}$	SCSC	+++
$RcsF_{C109/C124S}$	CSCS	−

Cys^{109}–Cys^{124} Disulfide Is Required for Assembly—A striking feature of the RcsF structure is the presence of two nonconsecutive disulfides. We wanted to determine whether these disulfides are required for activation of the Rcs phosphorelay. We generated single cysteine to serine mutants and tested whether expression of the mutants in the periplasm leads to a mucoid phenotype (Table 2 and supplemental Fig. S2). We observed that expression of $RcsF_{C74S}$ and $RcsF_{C118S}$, in which only the Cys^{109}–Cys^{124} disulfide remains, leads to a mucoid phenotype. In contrast, expression of the $RcsF_{C109S}$ and $RscF_{C124S}$ mutants, in which only the Cys^{74}–Cys^{118} disulfide can be formed, does not activate the production of capsule polysaccharides (Table 2). Similar results were obtained when the cysteine pairs Cys^{74}–Cys^{118} and Cys^{109}–Cys^{124} were mutated; only expression of an RcsF mutant, in which Cys^{74} and Cys^{118} are replaced by serines (this mutant conserves the Cys^{109}–Cys^{124} disulfide), resulted in a mucoid phenotype (Table 2). The mutated proteins in which the Cys^{109}–Cys^{124} disulfide cannot be formed were not detected by Western blot analysis, in contrast to the mutants lacking the Cys^{74}–Cys^{118} disulfide (data not shown). This suggests that the inability of the mutant proteins lacking the Cys^{109}–Cys^{124} disulfide to activate the phosphorelay is due to a folding defect. Thus, these experiments suggest that the Cys^{109}–Cys^{124} disulfide is important for the assembly of an active RcsF in the cell envelope, whereas the Cys^{74}–Cys^{118} disulfide seems to be dispensable.

dsbC Deletion Prevents Signaling through RcsF—In *E. coli*, disulfides are introduced into periplasmic proteins by the oxidoreductase DsbA (37). The dependence of RcsF on DsbA for oxidative folding has already been reported by Kadokura *et al.* (38) and was not explored further in this work. DsbA is a pow-

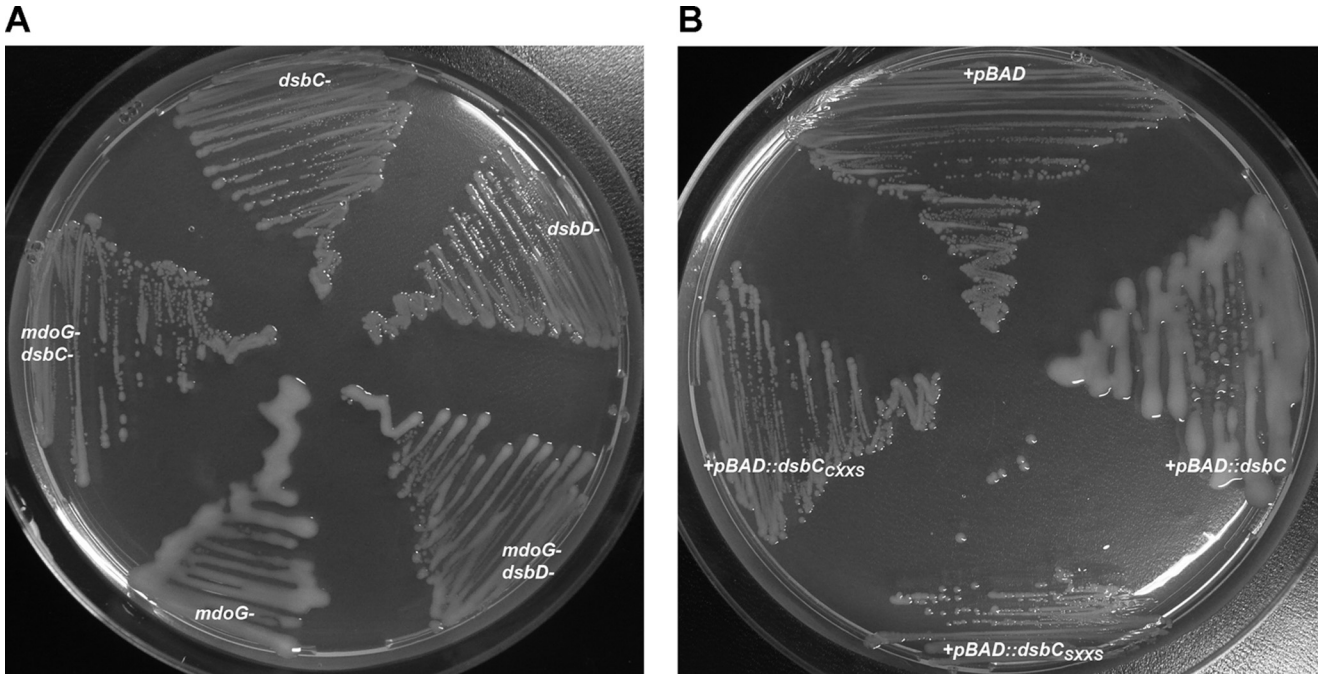

FIGURE 4. **Deletion of *dsbC* prevents the induction of the Rcs phosphorelay by deletion of *mdoG*.** *A, mdoG, dsbC, dsbD, mdoG dsbC,* and *mdoG dsbD* mutant strains were grown on M63 minimal medium for 2 days at room temperature. Similar results were obtained for the *mdoH* mutants (data not shown). *B, mdoG dsbC* strain was complemented with either pBAD33, pBAD33::*dsbC*, pBAD33::*dsbC*$_{CXXS}$, or pBAD33::*dsbC*$_{SXXS}$ and grown on M63 minimal medium for 2 days at room temperature. Like DsbC$_{SXXS}$, DsbC$_{CXXS}$ keeps the chaperone activity but cannot function as reductase.

erful oxidant that rapidly reacts with unfolded proteins to oxidize them (37, 39). When disulfides need to be formed between cysteine residues that are not consecutive in the sequence, as is the case in RcsF, DsbA may introduce non-native disulfides, which leads to protein misfolding and proteolysis. These non-native disulfides are corrected by DsbC, a soluble dimeric protein that functions as a protein-disulfide isomerase in the periplasm (39, 40). Each monomer of DsbC possesses a thioredoxin domain harboring a catalytic C*XX*C motif. The cysteine residues of this motif are kept reduced in the periplasm by DsbD, an inner membrane protein that catalyzes the transfer of reducing equivalents from the cytoplasmic thioredoxin system across the membrane to DsbC (41). These reducing equivalents maintain DsbC in a reduced state in the periplasm, allowing the protein to function as an isomerase/reductase (see below). Several DsbC substrates with multiple cysteines have already been identified; they include four periplasmic enzymes (42, 43) as well as the essential β-barrel protein LptD (44).

The presence of two disulfides formed between cysteines that are not consecutive in the sequence of RcsF suggested that the assembly of this protein involves DsbC. To test this hypothesis, we searched to determine whether deletion of *dsbC* affects signaling via RcsF. As explained in the Introduction, it has been reported that mutations that alter the integrity of the cell envelope, such as *mdoG* and *mdoH*, induce the Rcs phosphorelay in an RcsF-dependent manner (19). We generated double mutants *mdoH dsbC* and *mdoG dsbC* to determine whether deletion of *dsbC* alters the mucoid phenotype of single mutants *mdoH* and *mdoG*. We found that whereas the *mdoG* and *mdoH* strains appear mucoid on minimal media, in agreement with reported data, the double mutants do not (Fig. 4*A*). This indicates that deletion of *dsbC* prevents the induction of the Rcs phosphorelay via RcsF and suggests that RcsF assembly involves DsbC.

The nonmucoid phenotype of the double mutants could result from the absence of the isomerase activity of DsbC or from the absence of the chaperone activity of DsbC, which has been described *in vitro* (45). To test these two hypotheses, we studied the phenotype of *mdoG dsbD* and *mdoH dsbD* double mutants. In strains lacking *dsbD*, DsbC is not recycled and is mostly found in the oxidized state (46), which prevents the protein from functioning as an isomerase/reductase but does not affect the chaperone activity. We found that the double mutants *mdoG dsbD* and *mdoH dsbD* are less mucoid than the single mutants *mdoG* and *mdoH* (Fig. 4*A*), suggesting that it is the isomerase activity of DsbC that is important for RcsF assembly. However, in contrast to the deletion of *dsbC*, the deletion of *dsbD* did not completely abolish the production of colanic acid, which prevented us from clearly discriminating between the two hypotheses. Thus, to firmly establish the involvement of the isomerase activity of DsbC in RcsF assembly, we compared the ability of wild-type DsbC and of a DsbC mutant that lacks the isomerase activity but keeps the chaperone activity (DsbC$_{SXXS}$) to restore the mucoid phenotype of the double mutant *mdoG dsbC*. As shown in Fig. 4*B*, we observed that only expression of wild-type DsbC was able to restore the induction of the Rcs phosphorelay in the double mutant, indicating that it is the isomerase activity of DsbC that is involved in the assembly of RcsF.

RcsF Interacts with DsbC in Vivo—This prompted us to further investigate the interaction between RcsF and DsbC. As explained above, the catalytic site of DsbC is maintained in a reduced state in the oxidizing environment of the periplasm, which is critical to allow DsbC to react with non-native disul-

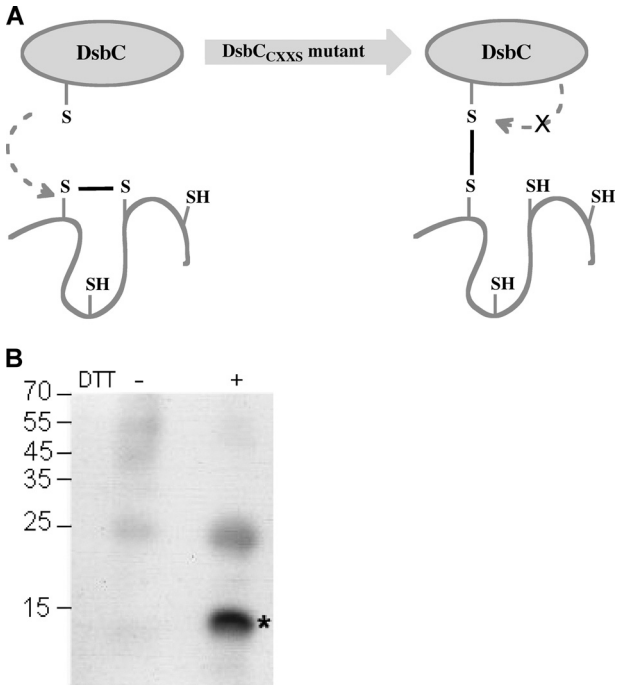

FIGURE 5. **Identification of RcsF trapped in complex with DsbC.** *A,* the first cysteine residue of the C*XX*C motif of DsbC performs a nucleophilic attack on an incorrect disulfide, which results in the formation of a mixed disulfide complex. To trap DsbC substrates, the C-terminal cysteine was replaced by a serine. This mutant protein is still able to react with non-native disulfides but lacks the second cysteine of the catalytic motif required to resolve the mixed disulfide complex. *B,* complexes formed between DsbC$_{CXXS}$ and its substrates were purified using Ni-NTA resin. The samples were analyzed by SDS-PAGE without or with DTT. RcsF was detected by Western blot using an anti-RcsF antibody. The band marked by an *asterisk* corresponds to RcsF that was released from the mixed disulfide complex with DsbC upon DTT addition.

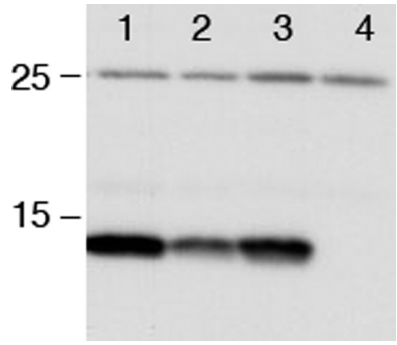

FIGURE 6. ***In vivo* expression levels of RcsF.** The RcsF expression level was determined in different backgrounds (*line 1,* wild type; *line 2, dsbC*; *line 3, dsbD*; *line 4, rcsF*). Cells were grown to exponential phase at 30 °C in M63 minimal medium, normalized by absorbance, and precipitated by TCA. RcsF was detected by Western blot using an anti-RcsF antibody.

fides. The first cysteine of the C*XX*C catalytic motif performs a nucleophilic attack on an incorrect disulfide, which results in the formation of an unstable mixed disulfide complex between DsbC and the substrate protein. There are two ways to resolve this mixed disulfide, either by attack of another cysteine of the misfolded protein, which results in the formation of a more stable disulfide in the substrate and the release of reduced DsbC, or by attack of the other cysteine of the C*XX*C motif. In this second case, DsbC is released in the oxidized state and functions as a true reductase.

To confirm that DsbC is involved in the assembly of RcsF, we expressed a mutated version of DsbC presenting a C*XX*S catalytic site (DsbC$_{CXXS}$) in a *dsbC* strain. Replacing the second cysteine of the catalytic site by a serine is a favorite approach to trap the complexes formed between the proteins from the thioredoxin family with their substrates (47, 48). As explained above, the C-terminal cysteine of the C*XX*C motif is the residue that performs a nucleophilic attack on the mixed disulfides formed between DsbC and its substrates. Thus, replacing this cysteine by a serine stabilizes the mixed disulfides and prevents DsbC from functioning as a reductase (Fig. 5*A*). After expression of the mutant protein in the periplasm of a *dsbC* deletion strain, the proteins were precipitated with TCA, and all free cysteines were alkylated with iodoacetamide to prevent any further disulfide bond rearrangements. The proteins were resuspended in a buffer containing 0.3% SDS and no reductant to maintain DsbC$_{CXXS}$ covalently bound to its potential substrate proteins. DsbC$_{CXXS}$ was then purified under denaturing conditions using a His tag present at the C terminus of the protein. Only one peak eluted from the column when an imidazole gradient was applied. DsbC was the most abundant protein in that peak, but other proteins of higher molecular weight were also present (data not shown). As the purification was performed under denaturing conditions, nonspecific binding to the column was minimal, and the bands co-eluting with DsbC likely correspond to complexes between DsbC and other proteins. To determine whether RcsF was trapped in complex with DsbC, the fractions were analyzed by Western blot using an anti-RcsF antibody. Although a band corresponding to the DsbC-RcsF complex could not be clearly identified (see under "Discussion"), we observed that addition of DTT led to the appearance of a band recognized by the anti-RcsF antibody and migrating at the size expected for RcsF (~14 kDa) (Fig. 5*B*). This indicates that RcsF forms a mixed disulfide complex with DsbC, and thus that RcsF interacts with DsbC *in vivo*.

Deletion of dsbC Decreases the Levels of RcsF in the Cell Envelope—We then sought to determine whether the deletion of *dsbC* affects the assembly of RcsF *in vivo* by comparing the levels of RcsF in wild-type and *dsbC* strains. As shown in Fig. 6, we observed that deletion of *dsbC* decreases the abundance of RcsF indicating that the absence of DsbC impairs the correct assembly of RcsF in the cell envelope. Deletion of *dsbD* also led to decreased RcsF levels, although to a lesser extent than the deletion of *dsbC*, which is in agreement with the mild mucoid phenotype exhibited by the *mdoG dsbD* mutant.

DISCUSSION

The Rcs phosphorelay plays an important role in the response of bacteria to envelope stress by controlling the transcription of many genes, including the cell division gene *ftsZ*, the catalase *katE*, and those involved in capsule synthesis, biofilm formation, and virulence factors (9). About 30 years of research on the Rcs phosphorelay have led to the identification of the major components of this system and the characterization of the activation cascade. However, surprisingly little is known about the molecular mechanisms that activate the system and fine-tune its activity in response to changes in the integrity of the cell envelope. One of the most fascinating questions is how the outer membrane lipoprotein RcsF is activated

and how, upon activation, it transmits the signal to the histidine kinase sensor RcsC, which is localized in the inner membrane. Biochemical and structural data are required to elucidate the details of the molecular mechanisms that led to the activation of this complicated multicomponent system and that allow signal transduction from the cell envelope to the cytoplasm.

Here, we report the structure of RcsF. The fold of the protein is characterized by a central four-stranded β sheet, sandwiched by two α helices. A similar fold has already been described in several proteins. Representative examples include dodecin, a small (7 kDa) riboflavin-binding protein found in prokaryotes that assembles to hollow sphere-like dodecameric complexes (49, 50), and the Alzheimer peptide precursor protein whose copper-binding domain is a structural homologue to RcsF (51).

Previous work by Kadukora *et al.* (38) led to the identification of RcsF as a substrate for the thiol-oxidase DsbA, which indicated that at least two of the four cysteine residues of RcsF are disulfide-bonded. This is nicely confirmed by the structure of RcsF, in which two disulfides can be observed. Interestingly, these two disulfides are formed between cysteine residues that are not consecutive in the sequence, Cys^{74}–Cys^{118} and Cys^{109}–Cys^{124}. This suggested that the assembly of RcsF involves the periplasmic protein-disulfide isomerase DsbC. The involvement of DsbC in the formation of the RcsF disulfides was confirmed by a combination of genetic and biochemical evidence. 1) We showed that deletion of *dsbC* prevents the induction of the Rcs phosphorelay in *mdoG* and *mdoH* mutants, in which Rcs activation had been shown to occur through RcsF. 2) By using complementation experiments with wild-type DsbC or with a DsbC variant lacking the catalytic cysteine residues, we showed that it is the isomerase activity of DsbC that is important for RcsF assembly. 3) We showed that *dsbC* deletion leads to decreased levels of RcsF in the outer membrane. Furthermore, we observed that RcsF copurifies under nonreducing and denaturing conditions with a DsbC variant lacking the resolving cysteine of the C*XX*C. Addition of DTT to reduce the mixed disulfide linking DsbC to its target proteins led to the release of RcsF, which provides good evidence that these two proteins interact in the periplasm. The disulfide-bonded DsbC-RcsF complex (40 kDa) could not be clearly identified on the Western blot probably because of an altered migration and transfer of the RcsF-DsbC complex and of a decreased accessibility of the RcsF epitope(s) when RcsF is bound to the isomerase.

We also tested the functional role of the two nonconsecutive disulfides, which allowed us to conclude that the two disulfides of RcsF are not functionally equivalent; the Cys^{109}–Cys^{124} disulfide seems particularly important for the stability of the protein as attested by the fact that removal of this disulfide impairs the assembly of RcsF more significantly than removal of the Cys^{74}–Cys^{118} disulfide. Importantly, similar results were obtained independently by Prouvost (56) on *Erwinia chrysantemi* RcsF. In a recent publication, Farris *et al.* (22) generated mutants of *Salmonella enterica* serovar Typhimurium RcsF presenting cysteine to serine point mutations. They tested whether those RcsF mutants could activate the Rcs phosphorelay in response to polymyxin B, a cationic antimicrobial peptide, using a *wza*::*lacZ* transcriptional reporter (the *wza* gene is regulated by the Rcs system). In contrast to our results showing that RcsF mutants lacking the Cys^{74}–Cys^{118} disulfide are still able to signal, they report that no β-galactosidase activity was observed for any of the four point mutants. This discrepancy could result from the fact that they used *S. enterica* serovar Typhimurium RcsF as well as a different reporter of Rcs activation.

Recently, Singh *et al.* (52) determined the disulfide connectivity of RcsF to test a new mass spectrometry analysis method that they had designed. They found one disulfide between Cys^{74} and Cys^{124}. They deduced from that result that the second disulfide of RcsF connects Cys^{109}–Cys^{118}. They specifically searched their mass spectrometry data for this disulfide and found it. The structural and genetic data that we report indicate that, in contrast to what they found, RcsF contains two nonconsecutive disulfides between Cys^{74}–Cys^{118} and Cys^{109}–Cys^{124}. To determine whether other oxidized forms of RcsF were present in the sample that was used for crystallization, we analyzed the RcsF protein preparation by LC-MS/MS. Because RcsF has four cysteines, there are six different disulfides that can be formed. We found all the possible cysteine pairs in the sample (data not shown). However, using an internal standard, we quantified the various cysteine pairs and found that the Cys^{74}–Cys^{118} and Cys^{109}–Cys^{124} disulfides, which correspond to those observed in the structure of the native protein, represent more than 90% of the disulfide population. This suggests that the RcsF protein preparation that was used for crystallization is contaminated by low amounts of non-native RcsF presenting incorrect disulfides. Singh *et al.* (52) do not report any quantification results, which limits the interpretation of the data. However, it is likely that the disulfides that they identified correspond to those of a minor, non-native form of RcsF.

A striking feature of the disulfide connecting Cys^{109} and Cys^{124} is that it links two adjacent antiparallel β strands and thus occurs in a secondary structure that is already stabilized by hydrogen bonds. The Cys^{109}–Cys^{124} disulfide belongs to the category of the cross-strand disulfides (see the review by Wouters *et al.* (53) and references therein). CSD are relatively unusual. However, more and more structures presenting CSD have been deposited in the PDB over the past 10 years. For instance, CSD are found in the N-terminal domain (α domain) of DsbD, in the HIV-1 primary receptor CD4, and in ribonucleotide reductase. In most cases, CSD do not function as structure stabilizers but appear to play the role of a redox switch. Further studies are required to determine whether the CSD observed in RcsF also plays a functional redox role.

Acknowledgments—We thank Asma Boujtat and Steve Calberson for technical assistance and Matthieu Depuydt for critical reading of the manuscript. We thank the European Community for Access to Research Infrastructure Action of the Improving Human Potential Programme to the EMBL Hamburg Outstation, Contract RII3-CT-2004-506008.

REFERENCES

1. Bos, M. P., Robert, V., and Tommassen, J. (2007) *Annu. Rev. Microbiol.* **61,** 191–214
2. Leverrier, P., Vertommen, D., and Collet, J. F. (2010) *Proteomics* **10,** 771–784

3. Ruiz, N., Kahne, D., and Silhavy, T. J. (2006) *Nat. Rev. Microbiol.* **4,** 57–66
4. Ruiz, N., and Silhavy, T. J. (2005) *Curr. Opin. Microbiol.* **8,** 122–126
5. MacRitchie, D. M., Buelow, D. R., Price, N. L., and Raivio, T. L. (2008) *Adv. Exp. Med. Biol.* **631,** 80–110
6. Gottesman, S., Trisler, P., and Torres-Cabassa, A. (1985) *J. Bacteriol.* **162,** 1111–1119
7. Whitfield, C. (2006) *Annu. Rev. Biochem.* **75,** 39–68
8. Huang, Y. H., Ferrières, L., and Clarke, D. J. (2006) *Res. Microbiol.* **157,** 206–212
9. Majdalani, N., and Gottesman, S. (2005) *Annu. Rev. Microbiol.* **59,** 379–405
10. Laubacher, M. E., and Ades, S. E. (2008) *J. Bacteriol.* **190,** 2065–2074
11. Clarke, D. J. (2010) *Future Microbiol.* **5,** 1173–1184
12. Stout, V., and Gottesman, S. (1990) *J. Bacteriol.* **172,** 659–669
13. Clarke, D. J., Joyce, S. A., Toutain, C. M., Jacq, A., and Holland, I. B. (2002) *J. Bacteriol.* **184,** 1204–1208
14. Takeda, S., Fujisawa, Y., Matsubara, M., Aiba, H., and Mizuno, T. (2001) *Mol. Microbiol.* **40,** 440–450
15. Stout, V. (1994) *Res. Microbiol.* **145,** 389–392
16. Stout, V., Torres-Cabassa, A., Maurizi, M. R., Gutnick, D., and Gottesman, S. (1991) *J. Bacteriol.* **173,** 1738–1747
17. Wehland, M., and Bernhard, F. (2000) *J. Biol. Chem.* **275,** 7013–7020
18. Kelm, O., Kiecker, C., Geider, K., and Bernhard, F. (1997) *Mol. Gen. Genet.* **256,** 72–83
19. Castanié-Cornet, M. P., Cam, K., and Jacq, A. (2006) *J. Bacteriol.* **188,** 4264–4270
20. Gervais, F. G., and Drapeau, G. R. (1992) *J. Bacteriol.* **174,** 8016–8022
21. Hagiwara, D., Sugiura, M., Oshima, T., Mori, H., Aiba, H., Yamashino, T., and Mizuno, T. (2003) *J. Bacteriol.* **185,** 5735–5746
22. Farris, C., Sanowar, S., Bader, M. W., Pfuetzner, R., and Miller, S. I. (2010) *J. Bacteriol.* **192,** 4894–4903
23. Callewaert, L., Vanoirbeek, K. G., Lurquin, I., Michiels, C. W., and Aertsen, A. (2009) *J. Bacteriol.* **191,** 1979–1981
24. Majdalani, N., Heck, M., Stout, V., and Gottesman, S. (2005) *J. Bacteriol.* **187,** 6770–6778
25. Casadaban, M. J. (1976) *J. Mol. Biol.* **104,** 541–555
26. Miller, J. (1992) *A Short Course in Bacterial Genetics*, pp. 221–222, Cold Spring Harbor Laboratory Press, Cold Spring Harbor, NY
27. Datsenko, K. A., and Wanner, B. L. (2000) *Proc. Natl. Acad. Sci. U.S.A.* **97,** 6640–6645
28. Beck, T., Krasauskas, A., Gruene, T., and Sheldrick, G. M. (2008) *Acta Crystallogr. D Biol. Crystallogr.* **64,** 1179–1182
29. Kabsch, W. (1993) *J. Appl. Crystallogr.* **26,** 795–800
30. Panjikar, S., Parthasarathy, V., Lamzin, V. S., Weiss, M. S., and Tucker, P. A. (2005) *Acta Crystallogr. D Biol. Crystallogr.* **61,** 449–457
31. Murshudov, G. N., Vagin, A. A., and Dodson, E. J. (1997) *Acta Crystallogr. D Biol. Crystallogr.* **53,** 240–255
32. Collaborative Computational Project No. 4 (1994) *Acta Crystallogr. D Biol. Crystallogr.* **50,** 760–763
33. Emsley, P., and Cowtan, K. (2004) *Acta Crystallogr. D Biol. Crystallogr.* **60,** 2126–2132
34. Holm, L., and Rosenström, P. (2010) *Nucleic Acids Res.* **38,** W545–W549
35. Politzer, P., Lane, P., Concha, M. C., Ma, Y., and Murray, J. S. (2007) *J. Mol. Model* **13,** 305–311
36. Politzer, P., Murray, J. S., and Clark, T. (2010) *Phys. Chem. Chem. Phys.* **12,** 7748–7757
37. Depuydt, M., Messens, J., and Collet, J. F. (2011) *Antioxid. Redox. Signal.*, in press
38. Kadokura, H., Tian, H., Zander, T., Bardwell, J. C., and Beckwith, J. (2004) *Science* **303,** 534–537
39. Bardwell, J. C., McGovern, K., and Beckwith, J. (1991) *Cell* **67,** 581–589
40. Hiniker, A., and Bardwell, J. C. (2003) *Biochemistry* **42,** 1179–1185
41. Katzen, F., and Beckwith, J. (2000) *Cell* **103,** 769–779
42. Vertommen, D., Depuydt, M., Pan, J., Leverrier, P., Knoops, L., Szikora, J. P., Messens, J., Bardwell, J. C., and Collet, J. F. (2008) *Mol. Microbiol.* **67,** 336–349
43. Berkmen, M., Boyd, D., and Beckwith, J. (2005) *J. Biol. Chem.* **280,** 11387–11394
44. Denoncin, K., Vertommen, D., Paek, E., and Collet, J. F. (2010) *J. Biol. Chem.* **285,** 29425–29433
45. Chen, J., Song, J. L., Zhang, S., Wang, Y., Cui, D. F., and Wang, C. C. (1999) *J. Biol. Chem.* **274,** 19601–19605
46. Rietsch, A., Bessette, P., Georgiou, G., and Beckwith, J. (1997) *J. Bacteriol.* **179,** 6602–6608
47. Depuydt, M., Leonard, S. E., Vertommen, D., Denoncin, K., Morsomme, P., Wahni, K., Messens, J., Carroll, K. S., and Collet, J. F. (2009) *Science* **326,** 1109–1111
48. Collet, J. F., and Messens, J. (2010) *Antioxid. Redox. Signal.* **13,** 1205–1216
49. Grininger, M., Staudt, H., Johansson, P., Wachtveitl, J., and Oesterhelt, D. (2009) *J. Biol. Chem.* **284,** 13068–13076
50. Bieger, B., Essen, L. O., and Oesterhelt, D. (2003) *Structure* **11,** 375–385
51. Kong, G. K., Adams, J. J., Harris, H. H., Boas, J. F., Curtain, C. C., Galatis, D., Masters, C. L., Barnham, K. J., McKinstry, W. J., Cappai, R., and Parker, M. W. (2007) *J. Mol. Biol.* **367,** 148–161
52. Singh, P., Shaffer, S. A., Scherl, A., Holman, C., Pfuetzner, R. A., Larson Freeman, T. J., Miller, S. I., Hernandez, P., Appel, R. D., and Goodlett, D. R. (2008) *Anal. Chem.* **80,** 8799–8806
53. Wouters, M. A., Fan, S. W., and Haworth, N. L. (2010) *Antioxid. Redox. Signal.* **12,** 53–91
54. Bond, C. S. (2003) *Bioinformatics* **19,** 311–312
55. Potterton, L., McNicholas, S., Krissinel, E., Gruber, J., Cowtan, K., Emsley, P., Murshudov, G. N., Cohen, S., Perrakis, A., and Noble, M. (2004) *Acta Crystallogr. D Biol. Crystallogr.* **60,** 2288–2294
56. Prouvost, A. F. (2008) *Rôle du Périplasme dans la Perception par la Bactérie de son Environnement: Utilisation des β-Galactanes par Erwinia chrysanthemi: Voie de Signalisation du Système Rcs dans la Virulence d'Erwinia chrysanthemi*. Doctoral dissertation, Universite des Sciences et Technologies de Lille, Lille, France